THE ASTROPHYSICAL JOURNAL SUPPLEMENT SERIES, 34:405–423, 1977 July

MODELS OF INTERSTELLAR CLOUDS. I. THE ZETA OPHIUCHI CLOUD

J. H. BLACK
School of Physics and Astronomy, University of Minnesota
AND
A. DALGARNO
Center for Astrophysics, Harvard College Observatory and Smithsonian Astrophysical Observatory
Received 1976 October 8

ABSTRACT

Techniques for constructing detailed models of diffuse interstellar clouds are described. The models are designed to reproduce the observational data on the abundance and rotational excitation of H_2, the abundances of other molecules and of atomic ions, and the fine-structure populations of carbon. Results are presented for the ζ Ophiuchi cloud. A model with two components accounts adequately for all the available observational data. The temperature and total density are respectively 110 K and 500 cm^{-3} in the outer region and 22 K and 2500 cm^{-3} in the inner core. The measured abundance of CH can be reproduced by postulating a rate coefficient of 5×10^{-16} cm^3 s^{-1} at 22 K for the radiative association reaction $C^+ + H_2 \rightarrow CH_2^+ + h\nu$. The measured abundances of HD and OH can be reproduced by an ionization rate of 1.6×10^{-17} s^{-1} and a rate coefficient of 5×10^{-10} cm^3 s^{-1} for the reaction $O^+ + H \rightarrow O + H^+$. The abundances of CO and CN are reproduced by using plausible estimates of their photodissociation rates, but the chemical scheme seriously underestimates the abundance of CH^+. The concentrations of other simple molecules are predicted. The molecule C_2 may be detectable. The known heating sources appear adequate to maintain the inferred temperatures.

Subject headings: interstellar: matter — interstellar: molecules — nebulae: individual — molecular processes

I. INTRODUCTION

Detailed models of interstellar clouds are essential to the physical interpretation of observational data and to our understanding of the structure and evolution of the clouds. In this paper, we describe techniques for constructing complex models of diffuse interstellar clouds. The models are designed to take advantage of the wealth of ultraviolet line data from the Princeton spectrometer on the *Copernicus* satellite (Spitzer and Jenkins 1975).

The term "diffuse cloud" refers to a translucent absorbing region identifiable as a distinct interstellar line feature in the high-resolution spectra of background hot stars. Since the background stars in absorption line studies are effectively point sources, inhomogeneities in the intervening medium may be considered one-dimensional. In contrast to their dark-cloud counterparts, diffuse clouds are unlikely to contain hidden sources of heating, excitation, and ionization.

Models of interstellar clouds should be able to account for the amounts of atomic and molecular hydrogen, the abundances of simple molecules such as CH, CO, CN, and OH, the fractionation of HD, the degree of ionization of minor atomic species, and the populations of the rotational levels of the ground state of H_2. If a model can be constructed that reproduces the array of observational data, some confidence may be placed in the inferred physical parameters, such as the density, the temperature, the strengths of the ultraviolet radiation field, and the intensity of the ionization source. It is important that the abundances of the atoms, ions, and molecules be computed as functions of depth and integrated over path length since only column densities are directly measurable. The construction of a model thus involves the simultaneous treatment of the transfer of the photons which dissociate molecules, ionize atoms, and contribute to the heating; the chemical and ionization equilibria of the important constituents; and the statistical equilibrium describing level populations in H_2.

We illustrate the application of our techniques with a successful model of the best-studied diffuse cloud, that toward ζ Ophiuchi.

II. THE ABUNDANCE AND EXCITATION OF H_2

Observations have demonstrated that H_2 is abundant in many diffuse clouds (Carruthers 1970; Smith 1973; Spitzer *et al.* 1973). The observed amounts of H and H_2 are in good qualitative agreement with the theory of Hollenbach, Werner, and Salpeter (1971), in which H_2 is in equilibrium between formation on grain

surfaces and destruction by fluorescent photodissociation. The details of the grain catalysis process have been discussed frequently; notably by Hollenbach and Salpeter (1970, 1971) and most recently by Allen and Robinson (1976) and Barlow and Silk (1976). In the conventional manner, we assume that the rate of formation of H_2 is limited by the frequency of collisions between H atoms and grains and by the efficiency of recombination on the surface. The former depends upon the densities of atomic hydrogen, $n(\mathrm{H})$, and of grains, $n(g)$, upon the average geometrical cross section of the grains, and upon the gas temperature T. The efficiency of recombination is a property of an unknown solid surface and can only be estimated (cf. Hollenbach and Salpeter 1971). In practice, the rate of formation of H_2 is written

$$n(\mathrm{H})n(g)k_1 = n(\mathrm{H})n(g)10^{-6}T^{1/2}k_f \ \mathrm{cm^{-3}\ s^{-1}}, \quad (1)$$

where uncertainties in grain size and recombination efficiency are absorbed by the dimensionless parameter k_f and the dependence of the thermal velocity of H upon T is retained explicitly. We make the usual assumption that the number density of grains is related to the total hydrogen density through

$$n(g) = 10^{-12}n = 10^{-12}[n(\mathrm{H}) + 2n(\mathrm{H_2})]. \quad (2)$$

Then for $T = 100$ K and $k_f = 1$, H_2 forms at a rate $10^{-17}nn(\mathrm{H})\ \mathrm{cm^{-3}\ s^{-1}}$ as suggested by Hollenbach, Werner, and Salpeter (1971). Another source of H_2 is associative detachment of H^-:

$$\mathrm{H^- + H \rightarrow H_2 + } e \quad (3)$$

(McDowell 1961), and it has been included in the present models. It is a very minor source in general and not likely to contribute significantly in regions where large amounts of the molecule are observed (Dalgarno and McCray 1973).

Formation of H_2 is assumed to be in equilibrium with its destruction by ultraviolet photons and by cosmic rays. In diffuse clouds, H_2 is most readily destroyed by the photons having wavelengths in the range $912 \leq \lambda \leq 1108$ Å through absorption in the Lyman and Werner lines followed by fluorescence to the vibrational continuum of the ground state (Stecher and Williams 1967; Dalgarno and Stephens 1970):

$$\mathrm{H_2} + h\nu \rightarrow \mathrm{H_2^*} \rightarrow \mathrm{H + H}. \quad (4)$$

Because the dominant dissociation mechanism is initiated by a line absorption, increasing optical depth in H_2 lines results in a decreasing rate of dissociation so that the H_2 in the outer part of a cloud shields the interior molecules. Destruction by cosmic ray protons,

$$\mathrm{H_2} + p \rightarrow \mathrm{H_2^+} + e + p, \quad (5)$$

$$\mathrm{H_2} + p \rightarrow \mathrm{H + H^+} + e + p, \quad (6)$$

$$\mathrm{H_2} + p \rightarrow \mathrm{H + H} + p, \quad (7)$$

has been discussed in the context of interstellar clouds by Solomon and Werner (1971) and by Glassgold and Langer (1973). The rates of processes (5), (6), and (7) depend upon the efficiency of secondary ionizations and are taken to have values of $0.98\ \xi_0$, $0.02\ \xi_0$, and $0.1\ \xi_0\ \mathrm{s^{-1}}$, respectively (Solomon and Werner 1971; Cravens 1974), and are assumed to be independent of depth in diffuse clouds.

Because the principal depth-dependent variable is the rate of fluorescent dissociation of H_2, it is convenient to base the cloud models upon a depth scale having discrete steps in column density of H_2, $N(\mathrm{H_2})$. A careful treatment of the transfer of radiation in the Lyman and Werner lines is needed to obtain an accurate profile of the relative atomic and molecular concentrations. The rate of absorption in a single line, i, at a depth τ into the cloud can be written

$$R_i = \frac{W_i(\tau)\phi_c(\nu_i, \tau)}{N_i(\tau)}\ \mathrm{s^{-1}}. \quad (8)$$

The index i stands for all the quantum numbers which designate a specific transition at frequency ν_i, and $N_i(\tau)$ is the column density at depth τ of molecules in the lower state of transition i:

$$N_i(\tau) = \int_0^\tau n_i(x)dx\ \mathrm{cm^{-2}}. \quad (9)$$

The equivalent width $W_i(\tau)$ of the line at depth τ is defined in terms of $\phi_i(\nu, \tau)$ and $\phi_c(\nu, \tau)$, the intensities in the line and neighboring continuum, respectively, by

$$W_i(\tau)\phi_c(\nu, \tau) = \int_0^\infty (\phi_c - \phi_i)d\nu. \quad (10)$$

It is assumed that any continuous opacity does not vary with frequency across a line profile. The intensities are understood to be mean intensities averaged over angle. The specific intensity in the continuum, $I_\nu(\tau, \mu)$ may be found in terms of the boundary intensity, $I_\nu(0, \mu)$, incident upon a semi-infinite, plane-parallel medium by solving the appropriate equation of radiative transfer,

$$\frac{dI_\nu(\tau, \mu)}{d\tau} = I_\nu(\tau, \mu) - \frac{1}{2}\int_{-1}^{1} P(\mu, \mu')I_\nu(\tau, \mu')d\mu'. \quad (11)$$

We consider the case of nonconservative, isotropic scattering in which the scattering phase function is independent of angle and equal to the albedo,

$$P(\mu, \mu') = \tilde{\omega}. \quad (12)$$

If the medium has no internal sources of radiation, then equation (11) has a solution of the form

$$I_\nu(\tau, \mu) = g(\mu)\exp(-k\tau). \quad (13)$$

Inserting equation (13) into equation (11) results in

$$-k\mu g(\mu)\exp(-k\tau) = g(\mu)\exp(-k\tau) - \tfrac{1}{2}\tilde{\omega} \times \int_{-1}^{1} g(\mu')\exp(-k\tau)d\mu' . \quad (14)$$

Hence

$$\tfrac{1}{2}\tilde{\omega}\int_{-1}^{1} g(\mu')d\mu' = g(\mu)(1 + k\mu) . \quad (15)$$

As shown by Chandrasekhar (1960), a function of the form

$$g(\mu) \propto (1 + k\mu)^{-1} \quad (16)$$

results in the following characteristic equation

$$\frac{k}{\log(1 + k)/(1 - k)} = \frac{\tilde{\omega}}{2} , \quad (17)$$

which has roots k. Equation (17) may be evaluated easily as a double-valued function $k(\tilde{\omega})$; however, one set of values is obviously unphysical.

The radiative transfer problem may, of course, be solved for other geometries and scattering phase functions. Walmsley (1973) has discussed simple approximations applicable to spherical geometry, and Sandell and Mattila (1975) have explored the effects of various albedos and strongly forward-scattering phase functions which enhance the ability of the ultraviolet photons to penetrate into clouds. Clouds of the sort considered here (visual extinction $A_v \lesssim 0.5$ to the center) are not thick enough to show severe effects due to a forward-peaked phase function. The grain properties adopted in our models are described in detail below.

Given that $k(\tilde{\omega})$ has been determined,

$$I_\nu(\tau, \mu) = \frac{A\exp(-k\tau)}{1 + k\mu} . \quad (18)$$

The quantity A is fixed by the boundary conditions, so that an isotropic external radiation field gives

$$I_\nu(0, \mu) = \phi_0(\nu) \qquad \mu \geq 0 ,$$
$$= A(1 + k\mu)^{-1} \quad \mu < 0 , \quad (19)$$

with the result that the corresponding mean intensity $\phi_c(\nu)$ is given by

$$\phi_c(\nu) = \phi_0(\nu)\exp(-k\tau) . \quad (20)$$

The nature of the boundary radiation field is discussed in § III.

The equivalent width in equation (8) can now be evaluated, either as an explicit integration over the line profile (10) or by use of the curve of growth in which $W_i(\tau)$ is a function of the column density of absorbers $N(\tau)$. For these computations involving a large number of lines and many depth steps, the use of curves of growth is much more expedient. Rodgers and Williams (1974) have suggested a simple approximation for the integrated absorption of a spectral line having a Voigt profile. The maximum error in this approximation is 8%, which is entirely satisfactory in a physical application fraught with far more severe inherent uncertainties. In this way it is possible to evaluate speedily and explicitly the equivalent widths in all lines at every depth point.

So far only a single, isolated line has been considered. Care must be taken in evaluating the absorption rates when lines overlap. It can be shown that the relevant lines of H, H_2, and HD generally overlap severely only in the wings. In this case we suggest a simple approximation in which line overlap is treated as an additional continuous opacity.

In terms of the oscillator strength f_i, the integrated cross section is given by

$$\int_{-\infty}^{\infty} \sigma(\nu)d\nu = \frac{\pi e^2}{mc} f_i \text{ cm}^2 \text{ Hz} . \quad (21)$$

The line widths are due only to Doppler and natural broadening, and the absorption cross section becomes

$$\sigma(\nu) = \sigma_0 K(x, y) , \quad (22)$$

where

$$K(x, y) = \frac{y}{\pi}\int_{-\infty}^{\infty} \frac{\exp(-t^2)}{y^2 + (x - t)^2} dt \quad (23)$$

is the Voigt function, a convolution of Gaussian and Lorentzian profile functions, and x is the frequency relative to line center, ν_0, in units of the Doppler half-width

$$x = \frac{\nu - \nu_0}{\alpha_D}(\ln 2)^{1/2} . \quad (24)$$

The parameter α_D is defined as

$$\alpha_D = \frac{\nu_0}{c}\left[\frac{2kT}{M}(\ln 2)^{1/2}\right]^{1/2} , \quad (25)$$

where M is the molecular mass. Equation (25) is appropriate for strictly thermal broadening; if Gaussian turbulence is included, then

$$\alpha_D = 3.5825 \times 10^{-7}\nu_0[T/M + 40.4(\delta V)^2]^{1/2} , \quad (26)$$

with M measured in atomic mass units and ν_0 in Hz. The full width at half-maximum of the velocity distribution, δV, in km s^{-1} is related to the conventional Doppler parameter (the rms dispersion) by

$$b = \frac{\delta V}{2(\ln 2)^{1/2}} = 0.6006\,\delta V . \quad (27)$$

The parameter y in equation (23) is the ratio of natural to Doppler widths

$$y = \frac{\alpha_L}{\alpha_D}(\ln 2)^{1/2} , \quad (28)$$

where

$$\alpha_D = \frac{A_i^*}{4\pi} . \quad (29)$$

For H_2, A_i^* is the total probability of radiative transitions out of the upper state of line i, both to vibrational bound levels of the ground state and to vibrational continuum states. The Voigt function so defined is normalized so that

$$\int_{-\infty}^{\infty} K(x, y)dx = \pi^{1/2} . \quad (30)$$

Thus

$$\sigma(\nu) = 0.012466 K(x, y) f_i \alpha_D^{-1} . \quad (31)$$

If we define for line i the quantities

$$\alpha_i = \alpha_D(\ln 2)^{-1/2} \quad (32)$$

and

$$\beta_i = \frac{e^2}{mc} f_i , \quad (33)$$

then in the line wings,

$$\sigma_i(x) \approx \frac{\beta_i}{\alpha_i} \frac{y_i}{x^2} . \quad (34)$$

Consider a nearby line j. As long as the separation greatly exceeds the Doppler width of either line,

$$\chi_{ij} = \left| \frac{\nu_j - \nu_i}{\alpha_i} \right| \gg 1 , \quad (35)$$

then the average absorption cross section due to line i in the vicinity of line j is, to a good approximation,

$$\bar{\sigma}_{ij} = \frac{\alpha_i \int_{x_{ij}-a}^{x_{ij}+a} \sigma_i(x)\, dx}{2a\alpha_j} \quad (36)$$

$$= \frac{\beta_i y_i}{2a\alpha_j} \left| \frac{2a}{x_{ij}^2 - a^2} \right| . \quad (37)$$

Because of equation (35), the effective extent of the line, a, must satisfy $a \ll x_{ij}$ so that

$$\bar{\sigma}_{ij} \approx \frac{\beta_i y_i}{\alpha_j x_{ij}^2} . \quad (38)$$

In general, for each line j, it suffices to consider the effect due to the one closest line i.

The total optical depth, τ, in equation (8) is a combination of extinction by grains, continuous absorption due to photoionization of atoms and molecules (notably atomic carbon), and the line overlap absorption. It can be shown that resonant scattering in the H_2 lines has a negligible effect because there are so many longer wavelength fluorescent lines through which the radiation emerges without being reabsorbed by H_2, As a result, the effective albedo in equation (12) may be written simply in terms of the grain albedo, $\tilde{\omega}_g$:

$$\tilde{\omega} = \frac{\tilde{\omega}_g \tau_g(\nu)}{\tau(\nu)} . \quad (39)$$

By definition, the extinction optical depth, $\tau_g(\nu)$, is related to the corresponding extinction in magnitudes by

$$A_v = 1.086\, \tau_g(\nu) , \quad (40)$$

and the ratio $\tau_g(\nu)/A_v$ may be determined from the observed extinction curves (Bless and Savage 1972; York *et al.* 1973; Johnson and Borgman 1963). The visual extinction is assumed to be proportional to total column density (eq. [2]) which, for ζ Oph, gives

$$A_v = 7.4 \times 10^{-22}[N(\mathrm{H}) + 2N(\mathrm{H}_2)] . \quad (41)$$

Table 1 summarizes the grain properties used in the present work. It presents, as functions of wavelength, the ratio $\tau_g(\lambda)/\tau_g(v)$, where $\tau_g(v)$ is the grain opacity at 5500 Å; the grain albedo $\tilde{\omega}_g$; and the corresponding value of k from equation (17). The albedo used is consistent with the measurements of Witt and Lillie (1973).

The total rate of photodissociation of H_2 may be written

$$k_4 = \sum_i R_i \eta_i , \quad (42)$$

where the summation is over all absorption lines and the rate R_i is weighted by the relative population of the lower state of transition i. The relative probability, η_i, with which the upper level of the transition decays to the vibrational continuum of the ground state has

TABLE 1

ADOPTED GRAIN PROPERTIES

Wavelength (Å)	τ_λ/τ_v	$\tilde{\omega}$	$\kappa(\omega)$
900.....	6.30	0.90	0.534
1000.....	5.15	0.90	0.534
1100.....	4.10	0.90	0.534
1200.....	3.50	0.90	0.534
1300.....	3.00	0.90	0.534
1400.....	2.75	0.90	0.534
1500.....	2.60	0.90	0.534
1600.....	2.55	0.85	0.629
1700.....	2.50	0.78	0.738
1800.....	2.45	0.66	0.865
1900.....	2.45	0.50	0.957
2000.....	2.55	0.30	0.998
2100.....	2.80	0.19	1.000
2200.....	2.75	0.17	1.000
2300.....	2.50	0.17	1.000
2400.....	2.30	0.19	1.000
2500.....	2.20	0.33	0.995
2600.....	2.10	0.37	0.990
2700.....	1.95	0.41	0.983
2800.....	1.85	0.44	0.976
2900.....	1.80	0.46	0.970
3000.....	1.75	0.48	0.964
3100.....	1.65	0.49	0.960
3200.....	1.60	0.50	0.957

been calculated by Stephens and Dalgarno (1972). The rate of dissociation of HD may be evaluated in exactly the same manner. The total rate of dissociation of H_2 varies drastically as a function of depth due to self-shielding. As noted by Spitzer *et al.* (1973), the rate of dissociation of HD is less dependent on depth in diffuse clouds because its abundance is too low for the Lyman lines to become strongly self-shielding and because it is not shielded by H_2 due to the large isotope shifts of the absorption lines.

Figure 1 illustrates the rates of dissociation of H_2 and HD as functions of molecular column density for the ζ Oph cloud model described below. The precise shapes of these curves depend upon the variation of τ_g with $N(H_2)$ and also upon the velocity dispersion of the molecules. The rates of fluorescent excitation of H_2 in the nondissociative Lyman and Werner system transitions and of photoionization of carbon are shown in the same figure. The photoionization of carbon is particularly important because of its contribution to the electron concentration and because of the subtle effect of H_2 line absorptions in attenuating carbon-ionizing photons (Dalgarno and McCray 1972). The effect of H_2 on carbon ionization has been calculated explicitly, and its magnitude is also shown in Figure 1.

In practice, the temperatures and densities of the diffuse clouds with optically thick H_2 (cf. Jura 1975*b*) permit substantial populations of only the lowest rotational levels, $J = 0$ and $J = 1$ in H_2 and $J = 0$ in HD. Accordingly, 78 absorption lines of H_2 and 20 lines of HD must be considered in the explicit treatment of ultraviolet dissociation and excitation. The equilibrium populations of levels J of the $v'' = 0$ rotational ladder in H_2 are evaluated in a straightforward way. A given level is populated by collisional excitation of lower levels, by collisional de-excitation and radiative decay of higher levels, by cascade from excited rotation-vibration levels, and directly by molecule formation and fluorescence. The level loses population by collisional excitation and de-excitation to other levels, by spontaneous radiative transitions (if $J \geq 2$), and by ultraviolet absorption. These processes can be represented by a set of coupled linear equations which can be solved by conventional matrix inversion techniques. The theory of fluorescence and cascading in H_2 has been described in detail by Black and Dalgarno (1976).

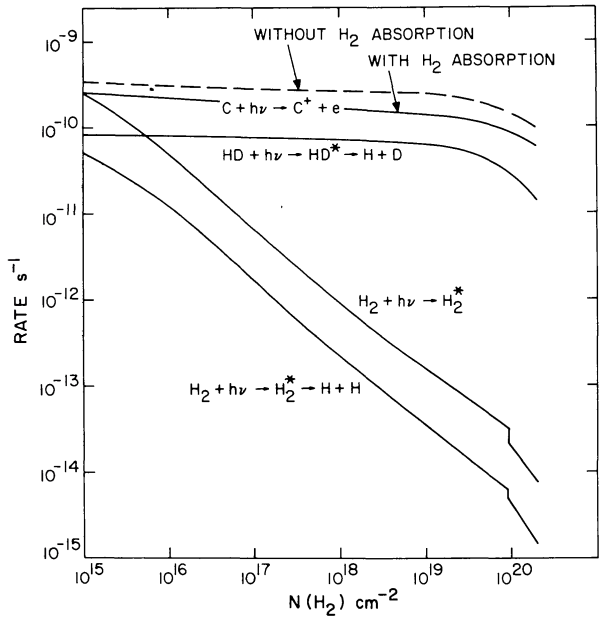

FIG. 1.—Rates of photodissociation of H_2 and HD, of nondissociative excitation of H_2, and of photoionization of C are shown as functions of column density of H_2. The effect of H_2 lines upon carbon ionization is indicated.

Rotationally inelastic collisions of H_2 with H, H_2, He, and electrons are important in the statistical equilibrium calculation. Although the process

$$H + H_2(J = 0) \rightarrow H_2(J = 2) + H \qquad (43)$$

has been studied extensively, uncertainties in the potential energy surface have led to large differences in the published cross sections. Calculations include the close-coupling results of Allison and Dalgarno (1967) and of Wolken, Miller, and Karplus (1972); the calculations in the distorted-wave Born approximation of Dalgarno, Henry, and Roberts (1966); and the application of the so-called modified wave-number approximation by Nishimura (1968). Chu and Dalgarno (1975*a*) have recently studied angular distributions in H–H_2 collisions.

Given the uncertainties in the interaction potential, there is not necessarily a clear choice among the various calculations, and experimental data on rotational relaxation times (e.g., Moraal and McCourt 1972) are not extensive enough to provide a complete set of rate coefficients.

The present cloud models incorporate sets of H–H_2 thermal rate coefficients based upon the cross sections of Allison and Dalgarno (1967) and of Wolken, Miller, and Karplus (1972). Where cross sections for transitions between the higher levels do not exist, we have estimated rate coefficients by assuming that the cross section for $J \rightarrow J + 2$ has the same dependence upon the ratio of impact energy to threshold energy as the cross section for $J \rightarrow 0 \rightarrow J = 2$. As long as the densities are high enough to effect thermalization of levels $J = 2$ and perhaps $J = 3$, the statistical equilibrium calculations are not very sensitive to the cross sections used, since the populations of levels $J \geq 4$ are normally dominated by cascade and radiative decay.

The adopted rates for H_2–H_2 collisions were based upon the work of Allison and Dalgarno (1967) and those for He–H_2 upon the calculations of Johnson and Secrest (1968) and McGuire and Micha (1972). More accurate cross sections have been reported recently by Green (1975). Cross sections for rotational excitation by electron impact are better determined, but electrons are also less important because of their low abundance in interstellar clouds. Since the lowest vibrational threshold of H_2 is at an energy large

compared with typical thermal energies, we have ignored vibrationally inelastic collisions.

It has been argued (Dalgarno, Black, and Weisheit 1973) that proton-interchange reactions permit levels $J = 0$ and $J = 1$ to be thermalized at low kinetic temperatures. In principle, the general process

$$H^+ + H_2(J) \leftrightarrow H_2(J + 1) + H^+ \qquad (44)$$

affects the rotational populations. To estimate the rate coefficients for equation (44), we assumed that the rate of de-excitation through interchange $J = 1 \rightarrow 0$ has a value 10^{-10} cm^3 s^{-1} independent of temperature. The other de-excitation rates $k(J + 1, J)$ are assumed to be related by

$$k(J + 2, J + 1) = \frac{2J + 3}{2J + 5} \frac{g(J + 1)}{g(J + 2)} k(J + 1, J), \qquad (45)$$

where $g(J)$ is the nuclear statistical weight, $g = 3$ or 1 when J is odd or even, respectively. The corresponding rates of excitation are calculated from detailed balance. With the explicit inclusion of the proton interchange process, the calculated ortho-para abundance ratio can vary with depth and will equal the thermal equilibrium value only if the proton density is large enough to maintain a high collision rate. Moreover, near the boundary of a cloud, the ultraviolet absorption rate may be large enough to dominate entirely the depopulation of the lowest levels and thus can destroy any semblance of thermal populations. For comparison with observation, of course, all level populations must be computed consistently as functions of depth and then integrated over path length to give column densities.

It should be emphasized that our model computations assume that the populations of the high rotational levels are maintained primarily by the radiative cascade following ultraviolet fluorescence and hot molecule formation (Black and Dalgarno 1976). Aannestad and Field (1973) presented an alternative explanation in which the excited molecules result from the passage of a shock through the gas at a velocity of the order of 5–10 km s^{-1}. While this mechanism may be important in certain regions, it appears not to be any more efficient than radiative cascading. In the specific case of the ζ Oph cloud, Morton (1975) has argued that the lack of observable velocity differences among H_2 lines arising in various levels appears to be contrary to the behavior expected in the shock model. More generally, the fluorescence and cascading which *must* accompany the photodissociation assumed by Aannestad and Field (1973) can maintain typical observed amounts of excited molecules even if the shock is not present. For example, the rate $k_4 = 10^{-14}$ s^{-1}, together with the preshock conditions $n(H) = 10$ cm^{-3}, $n(H_2) = 1$ cm^{-3}, and $T = 80$ K discussed by Aannestad and Field, leads to a population rate for level $J = 5$ of about $10^{-14} n(H_2)$ cm^{-3} s^{-1} by fluorescence and cascading. Since the radiative lifetime of level $J = 5$ is 10^8 s the implied concentration of $J = 5$ molecules in the absence of a shock is $10^{-6} n(H_2)$, a value generally consistent with the *Copernicus* observations of clouds having optically thick H_2.

III. CHEMICAL AND IONIZATION EQUILIBRIA

In this investigation, we have chosen to assemble a description of molecule formation based entirely upon gas-phase chemical reactions, with the single exception of the process of forming H_2. Such a theory makes many specific predictions and is therefore susceptible to observational tests. The content of the gas-phase scheme derives largely from the comprehensive study of molecule formation in dense clouds by Herbst and Klemperer (1973), although it differs in that it has been carried out specifically for the case of the diffuse clouds and thus includes calculations and estimates of photodestruction rates. In all, some 250 reactions involving about 65 molecular species are included in the chemical model. Because of the complexity of the chemical scheme and the availability of an appropriate review of the subject elsewhere (Dalgarno and Black 1976), only the dominant processes affecting the abundances of observable molecules will be discussed here.

A strong argument for the dominance of ion-molecule reactions is provided by the observations of HD (Spitzer *et al.* 1973) which requires a formation process much more rapid than that responsible for H_2 because of the shorter lifetime of HD in diffuse clouds. As suggested by Dalgarno, Black, and Weisheit (1973) and applied by Black and Dalgarno (1973*a*) and Watson (1973), the analog of the proton interchange reaction

$$D^+ + H_2 \rightarrow HD + H^+ \qquad (46)$$

dominates the formation of HD once H_2 is present. The deuterons arise primarily from charge transfer,

$$H^+ + D \rightarrow H + D^+, \qquad (47)$$

the principal source of free protons being reactions (6) and

$$H + p \rightarrow H^+ + e + p. \qquad (48)$$

The fractionation of deuterium thus depends upon the details of the transfer of dissociating photons for H_2 and HD and upon the equilibrium concentration of protons, which, in turn, is governed by the rate of cosmic ray ionizations. The concentration of OH is also related to the cosmic ray flux through the initiating reaction

$$H^+ + O \rightarrow O^+ + H, \qquad (49)$$

followed in molecular regions by

$$O^+ + H_2 \rightarrow OH^+ + H, \qquad (50)$$

$$OH^+ + H_2 \rightarrow H_2O^+ + H, \qquad (51)$$

$$H_2O^+ + H_2 \rightarrow H_3O^+ + H, \qquad (52)$$

$$H_3O^+ + e \rightarrow OH + H_2, \qquad (53)$$

or

$$H_3O^+ + e \rightarrow H_2O + H \quad (54)$$

and

$$H_2O + h\nu \rightarrow OH + H \quad (55)$$

(Black and Dalgarno 1973*a*; Watson 1973; Glassgold and Langer 1976). An alternative source also depending upon cosmic ray ionizations enters the above cycle at reaction (51) through

$$H_2^+ + H_2 \rightarrow H_3^+ + H\,, \quad (56)$$

$$H_3^+ + O \rightarrow OH^+ + H_2\,. \quad (57)$$

In addition to photodissociation,

$$OH + h\nu \rightarrow O + H \quad (58)$$

(Smith and Stella 1975; Smith and Zweibel 1976), OH is removed rapidly by C^+:

$$C^+ + OH \rightarrow CO + H^+ \quad (59)$$

or

$$C^+ + OH \rightarrow CO^+ + H\,. \quad (60)$$

These reactions are also likely to be the main source of CO, with the inclusion of two additional steps,

$$CO^+ + H_2 \rightarrow HCO^+ + H \quad (61)$$

and

$$HCO^+ + e \rightarrow CO + H\,. \quad (62)$$

Minor sources of CO include

$$CH^+ + O \rightarrow CO + H^+ \quad (63)$$

$$C_2^+ + O \rightarrow CO + C^+ \quad (64)$$

and a variety of neutral-neutral reactions such as

$$CH + O \rightarrow CO + H \quad (65)$$

$$CN + O \rightarrow CO + N\,. \quad (66)$$

CO is removed by

$$CO + h\nu \rightarrow C + O \quad (67)$$

and by

$$CO + He^+ \rightarrow C^+ + O + He\,. \quad (68)$$

The formation of the simple hydrocarbons can be initiated by radiative associations:

$$C^+ + H \rightarrow CH^+ + h\nu\,, \quad (69)$$

$$C + H \rightarrow CH + h\nu \quad (70)$$

(Bates and Spitzer 1951; Solomon and Klemperer 1972), but a larger source is

$$C^+ + H_2 \rightarrow CH_2^+ + h\nu \quad (71)$$

(Black and Dalgarno 1973*b*), followed by numerous reactions including

$$CH_2^+ + H_2 \rightarrow CH_3^+ + H\,, \quad (72)$$

$$CH_2^+ + e \rightarrow CH + H\,, \quad (73)$$

$$CH_3^+ + e \rightarrow CH_2 + H\,, \quad (74)$$

$$CH_2 + h\nu \rightarrow CH + H\,, \quad (75)$$

$$CH_2 + h\nu \rightarrow CH_2^+ + e\,, \quad (76)$$

$$CH + h\nu \rightarrow CH^+ + e\,, \quad (77)$$

$$CH^+ + H_2 \rightarrow CH_2^+ + H\,, \quad (78)$$

$$CH^+ + e \rightarrow CH + h\nu\,, \quad (79)$$

$$CH^+ + e \rightarrow C + H\,, \quad (80)$$

and photodissociation of molecular ions (Black, Dalgarno, and Oppenheimer 1975). As pointed out by Watson (1974), a related group of radicals may also be generated. Reactions of C^+ with CH, CH_2, and CH_3 form C_2^+, C_2H^+, and $C_2H_2^+$, respectively, which result in formation of C_2 and C_2H by

$$C_2H_2^+ + e \rightarrow C_2H + H \quad (81)$$

and

$$C_2H^+ + e \rightarrow C_2 + H\,. \quad (82)$$

The observation of interstellar absorption lines of C_2 would provide a very useful test of the chemical theory as shown in § V.

Nitrogen-bearing molecules are largely restricted to CN and HCN in diffuse clouds, and their abundances are tied closely to those of the simple hydrocarbon radicals through

$$CH^+ + N \rightarrow CN + H^+\,, \quad (83)$$

$$C_2^+ + N \rightarrow CN + C^+\,, \quad (84)$$

$$CH + N \rightarrow CN + H\,, \quad (85)$$

$$C_2 + N \rightarrow CN + C\,, \quad (86)$$

and by

$$CH_2^+ + N \rightarrow HCN^+ + H \quad (87)$$

and

$$CH_3^+ + N \rightarrow H_2CN^+ + H\,, \quad (88)$$

followed by

$$HCN^+ + e \rightarrow CN + H\,, \quad (89)$$

$$HCN^+ + H_2 \rightarrow H_2CN^+ + H\,, \quad (90)$$

$$H_2CN^+ + e \rightarrow HCN + H\,, \quad (91)$$

or directly through

$$CH_2 + N \rightarrow HCN + H\,. \quad (92)$$

The principal destruction mechanisms for HCN are sources of CN:

$$HCN + h\nu \rightarrow CH + H, \quad (93)$$

$$HCN + C^+ \rightarrow C_2N^+ + H, \quad (94)$$

$$C_2N^+ + e \rightarrow CN + C, \quad (95)$$

while CN itself is removed by

$$CN + h\nu \rightarrow C + N, \quad (96)$$

$$CN + O \rightarrow CO + N, \quad (97)$$

and

$$CN + He^+ \rightarrow C^+ + N + He. \quad (98)$$

The chemistry of chlorine species has been investigated by Jura (1974*a*) and Dalgarno *et al.* (1974), and is of particular interest because Cl, Cl^+, HCl, and HCl^+ have accessible spectral lines in the far-ultraviolet or visible.

An important feature of our cloud models is that the densities, temperatures, and radiation field which account for the concentration and excitation of H_2 are also required to reproduce the observed fractional ionization of atomic species. The situation is often complicated because large fractions of the higher stages of ionization may belong to ionized nebulae elsewhere along the line of sight to the background star. The problem is also complex for certain species whose ionization equilibria are affected by ion-molecule reactions.

The ionization of hydrogen is complicated. In addition to cosmic ray ionizations (reactions [6] and [48]) and radiative recombination,

$$H^+ + e \rightarrow H + h\nu, \quad (99)$$

the proton density is affected by charge transfer reactions with D, O, and various molecules, and can be augmented by the reverse of some charge transfer reactions and by such processes as

$$He^+ + H_2 \rightarrow H^+ + H + He, \quad (100)$$

$$D^+ + H_2 \rightarrow HD + H^+, \quad (101)$$

$$C^+ + OH \rightarrow CO + H^+, \quad (102)$$

and

$$CH^+ + O \rightarrow CO + H^+. \quad (103)$$

Helium ions are produced by cosmic rays and can participate in the chemistry through charge transfer and dissociative charge transfer with CO, H_2, CN, O_2, and N_2, and through a radiative charge transfer

$$He^+ + H \rightarrow H^+ + He + h\nu \quad (104)$$

(Jura and Dalgarno 1971).

Although carbon is ionized by readily available ultraviolet photons, its ionization equilibrium is affected by the presence of H_2 through

$$C^+ + H_2 \rightarrow CH_2^+ + h\nu \quad (105)$$

and through the competition for carbon-ionizing photons discussed above. Carbon ions also react readily with many other interstellar molecules. Similarly, the ionization of chlorine is affected by the rapid reaction

$$Cl^+ + H_2 \rightarrow HCl^+ + H. \quad (106)$$

Chemical reactions which might affect the ionization equilibria of minor species such as Fe, Si, S, Mg, and Al, although potentially important, will not be considered in detail here. For the minor elements only photoionization by photons with $\lambda > 912$ Å and radiative recombination are considered.

Rates for processes which depend upon the radiation field are discussed in the Appendix. The unattenuated background radiation field itself is taken to have the form

$$\phi_0(\nu) = 2.0 \times 10^{-17} \lambda^3 I \text{ photons cm}^{-2} \text{ s}^{-1} \text{ Hz}^{-1} \quad (107)$$

in the wavelength range 912–3300 Å where $\lambda = c/\nu$ is the wavelength in angstroms, and I is a scaling parameter such that the radiation energy density at 100 Å is 4×10^{-17} ergs cm^{-3} Å^{-1} (cf. Habing 1968) for $I = 0.5$. The flux used in the model computation is incident on each side of a plane-parallel cloud so that the energy density in the absence of the cloud would be twice the value obtained from equation (107). For $\lambda \geq 3300$ Å, the radiation field is represented by a diluted blackbody (Spitzer 1968) matched to the expression above.

It is both physically meaningful and computationally expedient to divide the full scheme of molecule formation into several families of reactions and species. These include the major constituents (H, H_2, H^+, D, and HD), the oxygen family (OH, H_2O, O_2), the carbon family (CH, CH^+, C_2, C_2H), the nitrogen family (NH, NH_3, N_2), and intermediate species such as CO, CN, HCN, and H_2CO which derive from more than one of the pure family groupings. The equations of chemical equilibrium have been solved iteratively on several levels according to the family groupings. Given approximations to the concentrations of the major constituents and initial estimates of the abundances of all other species, the equilibrium equations for each family have solutions which converge rapidly even in a first-order iteration scheme. It is then necessary to iterate upon the concentrations of the dominant species in each family and of the major intermediate species until overall convergence and mutual consistency are achieved.

IV. A MODEL OF THE ZETA OPHIUCHI CLOUD

As the first illustration of the application of the cloud models, we have chosen to develop a model of the major cloud component toward the star ζ Ophiuchi (HD 149757). The existing interstellar absorption line data for this region have been compiled and discussed by Morton (1975) in a study which combined the results of the classic paper by Herbig (1968) with those obtained from the Princeton ultraviolet spectrometer on

the *Copernicus* satellite. Additional *Copernicus* data have been discussed by de Boer *et al.* (1974), de Boer and Morton (1974), and Spitzer and Morton (1976). Since the appearance of Morton's (1975) paper, an additional important constituent of the cloud, OH, has been observed (Crutcher and Watson 1976; Snow 1976; Chaffee and Lutz 1976). The goal of the calculations was a model which would reproduce simultaneously the abundances of H and H_2, the populations of the excited rotational levels of H_2, the column densities of all the important atomic species, and the observed concentrations of HD, CO, CH, CN, and OH. A model which satisfies these criteria may then be used to examine the adequacy of known heating mechanisms in balancing the calculated cooling rates and to infer the primary cosmic ray ionization rate, ξ_0. It also provides predictions of the abundances of molecules which have not yet been observed directly.

The procedure begins with the computation of a family of models which all have the desired ratio of column densities $N(H)/N(H_2)$. Such a set of models is generally characterized by a particular value of the ratio $I/(nk_f)$. The population of one of the higher rotational levels, $J = 5$ or 6, relative to its ground state, $J = 1$ or 0, respectively, is usually sensitive to the quantity $n(I + k_f)$ over a wide range of physical conditions. The greatest contribution to the excited-state column densities tends to arise in the outer parts of the cloud where the rates of excitation and fluorescence (roughly proportional to nI) and of hot molecule formation (proportional to nk_f) are highest. The contribution of fluorescence and cascading to the excited-state populations reflects the relative concentrations in the lowest levels which are likely to be nearly thermalized at the kinetic temperature. The contribution of recently formed excited molecules to the cascade preserves the statistical populations appropriate to a very high effective formation temperature (cf. Black and Dalgarno 1976). Thus the values of I and k_f are related to the relative populations of the excited levels. This competition between the processes of ultraviolet fluorescence and molecule formation allows the ortho-para ratio to vary and explains why the relative populations of $J = 4$, 5, and 6 are *not* necessarily fixed once and for all by the nature of the cascade.

Calculation of the level populations is further complicated by allowance for total densities and temperatures, which vary as functions of depth. The *Copernicus* data commonly exhibit different excitation temperatures for populations of pairs of levels $J = 0$ and 1, 0 and 2, and 1 and 3 (Spitzer, Cochran, and Hirshfeld 1974). We suggest that this effect can in many cases be reconciled with simple models if the clouds have cold cores and hot outer layers. Morton (1975) has presented other observational arguments which support this contention for the ζ Oph cloud. In our model, it is necessary to have at least a two-phase structure in order to reproduce the relative populations of $J = 0$, 1, 2, and 3 to within the quoted observational uncertainties. We argue that the 1–3 excitation temperature is roughly the kinetic temperature of the hot layers, namely $T = 108$ K. The column density in $J = 0$ implied by this temperature is, of course, rather smaller than that observed, while the population of $J = 2$ comes into agreement with measurement. This suggests that the excess $J = 0$ population is confined to the cold core where the temperature is so low that levels $J = 1$, 2, and 3 are not significantly populated. The relative sizes of the hot and cold regions are thus determined; or, expressed in other terms, the discordant excitation temperatures may reflect primarily the temperature structure.

It is important to note that the atomic ionization equilibria are very sensitive to the temperature and density, and especially to the conditions in the cold core where the rates of radiative recombination are largest. In fact, the two-component models have proven to be far more successful than isothermal models in reproducing the observed concentrations of most atoms and their first ions. In the two-component models, the best agreement with observation is obtained with a rather smaller column-averaged density than in the case of single-component models. As a result, the very high densities suggested in our earlier preliminary calculations (Black and Dalgarno 1973*a*) are overestimates.

It is convenient to use the column density of H_2 as the fixed depth scale for the models because the rate of dissociation and hence the abundance of H_2 depends upon the column density of molecules available to provide shielding. The corresponding linear depth and total column density, $N = N(H) + 2N(H_2)$, are easily computed at each depth point once the concentrations of H and H_2 have been determined.

It is customary to compute a model only to the center of the cloud (corresponding to one-half of each column density) and to assume that both "sides" of the cloud are identical. For H_2, this approximation makes little difference; however, it is slightly less adequate for some atomic species. In any case, the uncertainties in the spectral character of the radiation field and of the optical properties of grains probably overshadow the limitations of the approximation.

Our final model of the cloud toward ζ Oph is characterized by $n = 500\ \mathrm{cm}^{-3}$ and $T = 110$ K in the outer zone and $n = 2500\ \mathrm{cm}^{-3}$ and $T = 22$ K in the inner zone. The outer zone has a linear size of $L = 1.71 \times 10^{18}$ cm and the inner zone has a size $L = 2.06 \times 10^{17}$ cm. The resulting total column density $N = 1.37 \times 10^{21}\ \mathrm{cm}^{-2}$ and total visual extinction $A_v = 1.01$ mag are in good agreement with observation. The intensity of the radiation field is given by $I = 2.50$, which is approximately twice the intensity of the general background in the direction of ζ Oph (Jura 1974*b*). The efficiency of formation of H_2 is $k_f = 2.86$, again a value which does not differ greatly from previous expectations (Hollenbach *et al.* 1971).

Morton (1975) has inferred a density of $n \gtrsim 10^4\ \mathrm{cm}^{-3}$ for the ζ Oph cloud based upon the ionization equilibria at an average temperature $T = 56$ K. De Boer and Morton (1974), on the other hand, have analyzed the populations of the fine-structure levels in C and

TABLE 2

MODEL OF ZETA OPHIUCHI CLOUD: RESULTS FOR HYDROGEN

Quantity	Observation	Total	Model Hot Zone	Model Cold Zone
N(H).....	20.72	20.73	20.701	19.544
$N(H_2)$ total....	20.62	20.62	20.246	20.38
$J=0$....	20.46	20.47	19.802	20.365
$J=1$....	20.10	20.07	20.040	18.897
$J=2$....	18.56	18.47	18.468	15.644
$J=3$....	17.07	16.94	16.940	14.90
$J=4$....	15.68	15.19	15.121	14.37
$J=5$....	14.63	14.75	14.704	13.75
$J=6$....	13.69	13.83	13.768	12.98
$J=7$....	13.55	13.58	13.53	12.64
$v=1$ $J=0$....	< 12.84	12.47	...	...
$v=1$ $J=1$....	< 13.08	12.90	...	...
$v=1$ $J=2$....	< 13.00	12.92	...	...
$v=2$ $J=0$....	< 12.64	12.13	...	...

have derived a density $n = 220$–$660\ \mathrm{cm}^{-3}$. This result, however, assumes that a relation between column densities, $N(\mathrm{H}) = 1.2\,N(\mathrm{H}_2)$, implies a similar relation between volume densities, $n(\mathrm{H}) = 1.2\,n(\mathrm{H}_2)$, at the particular depths where carbon is predominantly neutral. The strong depth-dependence of the molecular fraction almost certainly precludes such an assumption. Our two-component model resolves these apparent discrepancies. The greatest contribution to the column density of C occurs in the cold, dense core where $T = 22$ K. The recombination rate is thus larger than that adopted by Morton (1975). The observations are therefore consistent with lower $n(e)$ and n. We have computed the fine-structure excitation of C for a range of n and T using the cross sections of Yau and Dalgarno (1976) for excitation by H impact and find that the ζ Oph data are consistent with $n = 2500\ \mathrm{cm}^{-3}$ and $T = 20$ K, in agreement with the model of the central core. It is significant that $n(\mathrm{H}_2) \gg n(\mathrm{H})$ where most of the C exists. If fine-structure populations in C are to be useful diagnostics of conditions in such molecular clouds, the uncertainty about cross sections for excitation by H_2 must be removed by accurate calculations of the collision process. In the model, we have assumed that collisions with H are a constant factor of 10 times as efficient as collisions with H_2 in exciting fine structure in C.

The results of the model for hydrogen are compared with observation in Table 2. The measurements are from Morton (1975), with the addition of the improved column densities for H_2 in levels $J = 5$, 6, and 7 presented by Spitzer and Morton (1976). The contributions of the two zones are tabulated separately. Agreement with observation is quite good, and a more elaborate model incorporating continuously varying temperature and density would be needed only for minor improvements.

The depth dependences of the calculated rotational populations are illustrated in Figure 2. The density of H_2 in rotational level J, $n_J(\mathrm{H}_2)$, is presented as a function of the linear depth in centimeters. This depth scale shows clearly the contributions to column density. Because levels $J = 0$, 1, 2, and 3 are rather well thermalized, only $J = 0$ is populated substantially in the cold region while most of the H_2 in $J = 1$, 2, and 3 resides in the hot outer region. Although cascading at an enhanced total density continues to maintain populations in $J = 4$, 5, and 6, at least 85% of the column density in each of these excited levels derives from the outer regions where the rate of pumping is highest.

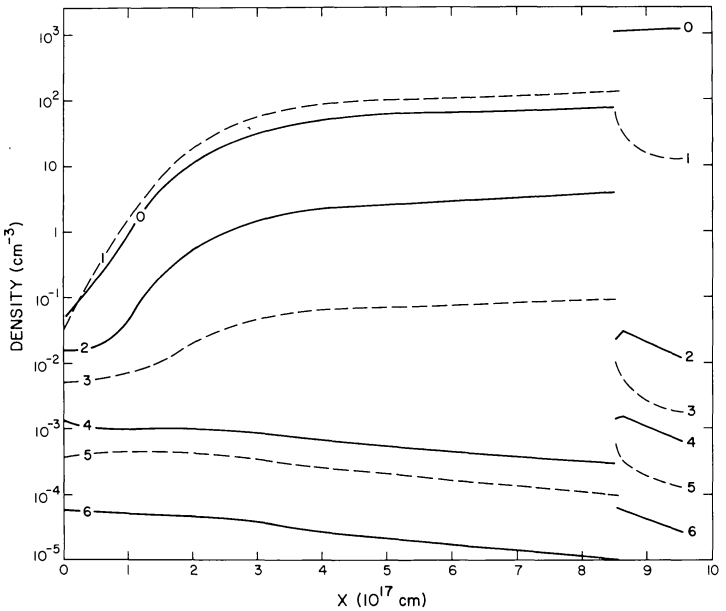

FIG. 2.—Densities of H_2 in rotational levels $J = 0$ through $J = 6$ are shown as functions of linear depth in the ζ Oph cloud model.

TABLE 3

ATOMIC COLUMN DENSITIES

Species	Observed	Calculated	$n(X)/n$	Depletion
Li.....	9.36	9.36	2.09 −10	0.19
C.....	15.56	15.60	9.25 −5	0.25
C^+.....	16.80–17.15	17.08		
N.....	16.22–16.70	16.48	2.23 −5	0.19
O.....	17.28–17.47	17.38	1.75 −4	0.26
Na.....	13.86	13.89	3.40 −7	0.20
Mg.....	14.15	13.92	1.55 −6	0.044
Mg^+...	14.91–15.27	15.31		
Al.....	< 10.21	9.35	1.31 −9	0.00052
Al^+....	12.09–12.41	12.25		
Si.....	< 12.58	12.24	8.22 −7	0.023
Si^+.....	14.80–15.30	15.05		
P.....	...	11.65	5.09 −8	0.19
P^+.....	13.74–13.92	13.84		
S.....	13.93	13.81	1.60 −5	1.00
S^+.....	15.86–16.24	16.34		
Cl.....	14.03	14.08	1.12 −7	0.25
Cl^+....	13.08–13.63	12.73		
K.....	11.90–12.39	12.15	2.75 −8	0.25
Ca.....	9.72	9.72	8.40 −10	0.00040
Ca^+....	11.64–11.73	11.84		
Ti.....	< 11.25	8.87	7.33 −11	0.0013
Ti^+.....	< 11.00	11.00		
Mn.....	< 11.58	11.72	1.23 −8	0.077
Mn^+...	13.26–13.33	13.21		
Fe.....	11.52	11.67	2.68 −8	0.0011
Fe^+....	14.48–14.64	13.56		

The agreement between theory and observation for the atomic abundances is at least as striking as the results for H_2. In Table 3, the observed and calculated column densities of neutral atoms and ions are compared, and the implied element abundances are tabulated. These results are generally in good agreement with the abundance determinations of Morton (1974) which are, of course, based upon the same observational data. As Morton (1974) has noted, the inferred depletions of most elements relative to solar-system values seem to be in harmony with Field's (1974) theory of element depletion, although alternative hypotheses (e.g., Snow 1975) may also require consideration. Where an element is observed in more than one stage of ionization, the calculated ionization balance is fairly accurate except for Fe. The spatial distributions of ions and neutrals will tend to be dissimilar, the neutral species being preferentially concentrated in the colder, denser core of the cloud. The column densities are thus sensitive to the details of the temperature and density profiles. These will, in some cases, be confused by the contribution of the H II region around the star itself. No attempt has been made here to separate carefully the contributions of neutral cloud and H II region to the column densities of ions. This problem has been treated in some detail by Steigman, Strittmatter, and Williams (1975), and we return to a discussion of it in § V. Finally, in our model the effects of chemical reactions upon the ionization equilibria have been included explicitly only for hydrogen, helium, carbon, nitrogen, oxygen, and chlorine.

The electron density computed for the model cloud ranges from $n(e) \approx 0.06\ \mathrm{cm}^{-3}$ in the warm outer component to $n(e) \approx 0.25\ \mathrm{cm}^{-3}$ in the cold core. Ionization of hydrogen contributes less than 10% of the electron density in the outer region and less than 1% throughout the core. The electrons arise predominantly from photoionization of C, Si, S, and Mg, as expected. The rate of photoionization of carbon remains high enough to maintain a fractional ionization of at least 90% throughout such a diffuse cloud. Even at the very center of the ζ Oph model, molecules contain only about 2% of the gas-phase carbon, although the reaction

$$C^+ + H_2 \rightarrow CH_2^+ + h\nu\,, \qquad (71)$$

followed by dissociative recombination of molecular ions, is only a factor of 5 less efficient in neutralizing C^+ than direct recombination,

$$C^+ + e \rightarrow C + h\nu\,. \qquad (108)$$

In clouds of somewhat greater extinction (column density) than the ζ Oph cloud, the ionization balance of species such as carbon will begin to be dominated by the ion-molecule chemistry (Oppenheimer and Dalgarno 1974).

The results of the chemical model are summarized in Table 4 with a tabulation of predicted column densities and observed values or upper limits. We have adopted the adjusted column density for OH, $N(\mathrm{OH}) = 5.1 \times 10^{13}\ \mathrm{cm}^{-2}$, suggested by Chaffee and Lutz (1977) as a reconciliation of the measurements of Snow (1976) and of Crutcher and Watson (1976). All the calculated column densities result from explicit integrations over path length of the concentrations predicted by the scheme of gas-phase molecule formation described above. The necessity of comparing observations with model column densities rather than with relative molecule concentrations computed at some average depth is demonstrated in Figure 3. The densities of the observed species H_2, HD, CO, CH, CN, and OH are shown as functions of $N(H_2)$ and of linear depth in the model. The depth at which the cold core region begins

TABLE 4

MOLECULE ABUNDANCES, LOG $N(X)$

Molecule	Observed	Predicted
HD.....	14.20	14.25
CO.....	15.03–15.20	15.02
CH.....	13.53	13.57
CH^+.....	12.97	11.39
CN.....	12.94	12.75
OH.....	13.71	13.69
H_2O.....	< 12.38*	12.03
C_2.....	< 12.72*	13.14
NH.....	< 13.87	9.02
HCl.....	< 12.97*	13.42
CO^+.....	< 12.76	9.83
NO^+.....	< 14.03	8.79

* Oscillator strength estimated; cf. Morton 1975.

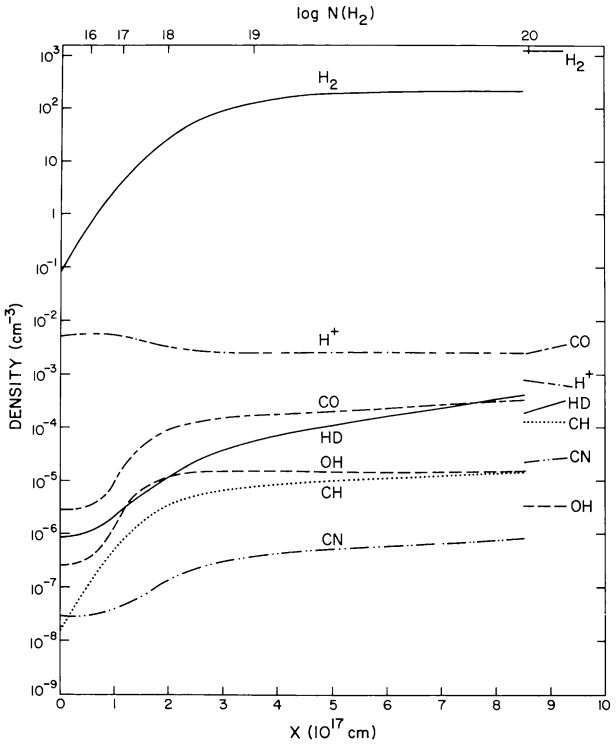

FIG. 3.—Computed densities of various molecules as functions of linear depth (*lower scale*) and of column density of H_2 (*upper scale*).

is of crucial importance for the major molecule abundances. CO, CH, and CN all show large abundance increases at the onset of higher density, while OH and HD exhibit decreases. The large decrease in OH concentration reflects the effect of enhanced density upon the proton density as well as the decreased temperature, which inhibits the initiating charge-transfer process. In contrast to the other observed species, the major contribution to the column density of OH occurs outside the cold core. The density of CN increases by a factor of 25, proportional to n^2, from outer to inner regions because its destruction is dominated by photodissociation, which does not change much with depth. CO, which is also removed by photodissociation, shows a more modest increase because its formation is tied to the OH abundance.

Since the abundances of both OH and HD depend upon the primary cosmic ray ionization rate, ξ_0, as discussed above, it should be possible to determine the value of ξ_0 from a model which reproduces the observed abundances of both (Black and Dalgarno 1973*a*). The problem is complicated by the uncertainty in the rate k_{49} of

$$H^+ + O \rightarrow O^+ + H\,. \qquad (49)$$

When ξ_0 and the rate, k_{109}, of

$$O^+ + H \rightarrow H^+ + O \qquad (109)$$

are taken as free parameters, the chemical model for the ζ Oph cloud indicates a narrow range of values of ξ_0 and k_{109} which reproduce simultaneously the observations of OH, HD, and CO. The results are

$$\xi_0 = 1.6 \pm 0.2 \times 10^{-17}\ \mathrm{s}^{-1} \qquad (110)$$

and

$$k_{109} = 4.9 \pm 0.6 \times 10^{-10}\ \mathrm{cm}^3\ \mathrm{s}^{-1}\,. \qquad (111)$$

The error limits reflect only the range of values in the model which result in correct molecular column densities. There are other sources of uncertainty in the calculation. If the reverse charge transfer (49) occurs at a rate

$$k_{49} = k_{109} \exp(-232/T) \qquad (112)$$

(Glassgold and Langer 1976), then $k_{49} = 4 \times 10^{-11}$ $\mathrm{cm}^3\ \mathrm{s}^{-1}$ at $T = 100$ K, a value which disagrees with the suggestion of Crutcher and Watson (1976) that this rate must be high to explain the amount of OH toward *o* Per.

Implicit in our analysis is the assumption of a standard deuterium abundance (Rogerson and York 1973; York and Rogerson 1976). Our determination of ξ_0 is consistent with the rate expected from the measured cosmic rays in the solar vicinity (Spitzer 1968), and it is in harmony with the upper limit of $10^{-16}\ \mathrm{s}^{-1}$ derived by O'Donnell and Watson (1974). Wright and Morton (1977) have recently determined that 13% of the HD toward ζ Oph is in the $J = 1$ level. Our model predicts the same fractional abundance.

A major uncertainty in the chemical scheme is the rate coefficient of the radiative association (reaction [71]). The ζ Oph model requires a rate $k_{71} = 5 \times 10^{-16}\ \mathrm{cm}\ \mathrm{s}^{-1}$, a result which is not unreasonable (cf. Dalgarno 1976), and indeed recent calculations by Herbst, Schubert, and Certain (1977) suggest a still higher value. Our adopted value provides excellent agreement between observed and predicted amounts of CH toward *o* Per and ζ Per in similar model calculations (Black, Dalgarno, and Hartquist 1977). The chemical scheme is also successful in predicting the abundances of CO and CN, the close agreement between theory and observation lending support to the photodissociation rates estimated by Solomon and Klemperer (1972).

A notable weakness of the chemical model is its failure to reproduce the observed high abundance of CH^+. Unless an important chemical reaction has been overlooked, the observed amounts of CH and CH^+ cannot coexist in the principal neutral cloud component. Perhaps the CH^+ belongs to a circumstellar region which does not contribute perceptibly to the column densities of H_2 and other prominent species in the dense neutral cloud. Zeta Oph itself is known to be losing mass and is likely to possess a fair amount of circumstellar matter (cf. Steigman, Strittmatter, and Williams 1975). The circumstellar environment may be unusual because the data of Abt and Biggs (1972) and Georgelin and Georgelin (1970) suggest that the star and its H II region, Sharpless 27, differ in radial velocity by 10 km s^{-1} or more.

TABLE 5

PREDICTED COLUMN DENSITIES OF UNOBSERVED SPECIES

Species X	log $N(X)$	Species X	log $N(X)$
O_2.....	11.15	N_2.....	13.03
CH_2.....	13.97	NH.....	10.14
CH_3.....	12.85	NH_2.....	7.26
CH_4.....	4.85	NH_3.....	6.76
CH_2.....	11.89	HCN.....	11.67
CH_3^+.....	12.58	HN_2^+.....	6.21
C_2.....	13.14	NO.....	11.54
C_2H.....	13.97	HCl^+.....	11.72
HCO.....	11.30	C_2^+.....	9.94
HCO^+.....	10.69	C_2H^+.....	10.79
H_2CO.....	10.93	$C_2H_2^+$.....	12.21
H^-.....	9.79		

Table 5 lists the predicted column densities of other molecular species in the calculation which have not yet been observed. Among these, perhaps C_2 stands the best chance of discovery. The equivalent widths of $R(0)$ lines in the Phillips and Mulliken systems, based upon a predicted column density of 1.4×10^{13} cm^{-2} of C_2 in $J = 0$ of the ground state, are presented in Table 6. Only one band in the Mulliken system is likely to be strong, and the oscillator strength has been measured by Smith (1969). The strengths of the Phillips system lines have been computed using the oscillator strength of Roux, Cerny, and d'Incan (1976) and the Franck-Condon factors of Spindler (1965). Detection of any of these lines at roughly the predicted strength would still be consistent with Morton's (1975) upper limit on the $F\,^1\Pi_u \leftarrow X\,^1\Sigma_g^+$ (0, 0) $R(0)$ line at 1341.63 Å as long as the unknown oscillator strength of that transition is less than 0.04. In any event, a careful search for one of the lines with a known oscillator strength may provide a useful test of the chemical model. The Phillips (4, 0) $R(0)$ line is very nearly coincident with a telluric line of O_2, but the other suggested interstellar lines appear to be free of such potential confusion. The predicted C_2 abundance is, however, sensitive to the photodissociation rate and to the rate coefficients of the chemical reactions that destroy C_2, and the uncertainties are large. The predicted abundance is probably an upper limit.

The predicted column densities of several other unobserved molecules are quite large. We note the abundances of CH_2, CH_3, and C_2H in particular. The spectra of CH_2^+, CH_3^+, and C_2H are essentially unknown. Observations of CH_2 and CH_3 would be very significant, although their ultraviolet transitions have a tendency to be weak and sometimes diffuse (Herzberg 1961).

The calculated column density of H_2CO relative to atomic hydrogen,

$$\frac{N(H_2CO)}{N(H)} = 1.6 \times 10^{-10}, \qquad (113)$$

is rather smaller than the value of 2×10^{-9} inferred for typical clouds by Davies and Matthews (1972) from observations of radio lines of H and H_2CO. The value predicted for a more extensive cloud ($A_v \gtrsim 1.5$ magnitudes) can be considerably larger due to an increase in the absolute abundance of H_2CO accompanied by a decrease in the relative column abundance of atomic hydrogen. The recent measurement of a low upper limit to the rate of

$$H_2CO^+ + H_2 \not\rightarrow H_3CO^+ + H \qquad (114)$$

has eliminated an attractive chemical path for forming H_2CO (Huntress 1977). Although the $^1A_2$–$^1A_1$ system of H_2CO has accessible lines near 3500 Å, the very small oscillator strength determined by diGeorgio and Robinson (1959) suggests an expected equivalent width no larger than 0.03 mÅ toward ζ Oph.

It is of interest to determine whether grain catalysis is capable of maintaining the observed abundances of simple molecules, particularly in the case of the simple hydrocarbons where our gas-phase theory hinges upon a postulated radiative association process (71). One approach to this question is to reduce the rate of the process (71) to $k_{71} = 10^{-18}$ cm^3 s^{-1} and to initiate the *known* experimentally studied parts of the gas-phase chemistry with a simulated grain catalysis process. We assume that the saturated molecule, CH_4, enters the gas from grain surfaces at a rate

$$n[n(C) + n(C^+)]k_x \text{ cm}^{-3} \text{ s}^{-1}.$$

TABLE 6

C_2: PREDICTED EQUIVALENT WIDTHS

Transition	Line	Wavelength Å	f	Equivalent Width (mÅ)
Mulliken $D\,^1\Sigma^+ \leftarrow X\,^1\Sigma_g^+$.....	0–0 $R(0)$	2312.160*	0.055	36
Phillips $A\,^1\Pi \leftarrow X\,^1\Sigma_g^+$.....	1–0 $R(0)$	10143.745†‡	0.0024	30
	2–0 $R(0)$	8757.66†	0.0013	13
	3–0 $R(0)$	7719.33†	0.00057	4.2
	4–0 $R(0)$	6912.70†	0.00021	1.2

* Wavelength in vacuo.

† Wavelength in air.

‡ Wavelength of the 1–0 transition has been computed from new molecular constants of Marenin and Johnson (1970) and corrected for standard atmospheric refraction. In all cases, designations of electronic states follow the suggested revisions of Herzberg, Lagerqvist, and Malmberg (1969).

The processes which destroy methane and convert it into other molecules have already been included explicitly. It makes little difference whether CH_4 or some other simple hydrocarbon is the direct product of the grain mechanism. The value of k_x was varied in the ζ Oph cloud model until the observed column density of CH was reproduced, with the result that k_x must equal 1.8×10^{-16} cm^3 s^{-1}. When cast into comparable form, the rate of formation of H_2 for the same model was $1.3 \times 10^{-17} n\, n(\mathrm{H})$ in the inner zone and $3 \times 10^{-17} n\, n(\mathrm{H})$ cm^{-3} s^{-1} in the outer zone. Thus hydrocarbon production would not only have to be far more efficient, but it would also need to proceed as a result of collisions of C^+ with grain surfaces. The requisite grain surfaces could not be positively charged. This requirement is in direct conflict with the current understanding of grain charge in diffuse clouds where photoemission of electrons from the surfaces is expected to be an efficient process. The photoemission is also an important heat source (Watson 1972; Jura 1976; de Jong 1977), and the problem of explaining the observed temperatures in diffuse clouds would be severely aggravated by these grain properties. The simulated grain catalysis mechanism results in substantial enhancements of the abundances of CH_3 and H_2CO, as indicated in Table 7. Observations of the Rydberg series bands of CH_3 in the far-ultraviolet could serve as a direct test of the two chemical schemes.

A major deficiency of the present model is that the thermal balance has not been calculated in a self-consistent fashion to produce a physically meaningful depth profile of temperature and total density. However, the contributions of known heating and cooling processes have been evaluated for the ζ Oph cloud model as a test of the adequacy of the heat sources. Cooling processes involving the abundant atomic and molecular species are very efficient in the temperature range $T = 20$–100 K, and the requirements on heat sources are rather severe. The presence of H_2 has several direct effects upon the thermal balance of diffuse clouds: pure rotational transitions in H_2 contribute to the cooling; H_2 is much less efficient than H in exciting the ground-state fine-structure transition in C^+, the dominant coolant (Chu and Dalgarno 1975*b*); and the conversion of a cloud from atomic to molecular hydrogen changes the total number of gas particles and hence the gas pressure, thus requiring some sort of adjustment of temperature and density to maintain hydrodynamic stability.

TABLE 7

SIMULATED GRAIN FORMATION OF SIMPLE MOLECULES

Molecules X	Gas Phase log $N(X)$	Grain Catalysis log $N(X)$
CH	13.57	13.60
CH_2	13.97	13.91
CH_3	12.85	13.59
CH_4	4.85	13.33
CH^+	11.39	11.62
CH_2^+	11.89	12.00
CH_3^+	12.58	12.55
CO	15.02	14.90
H_2CO	10.93	11.58
C_2H	13.97	13.89
C_2	13.14	13.08

The dominant cooling mechanisms in diffuse clouds are collisional excitation and radiative decay of low-lying fine structure in the ground states of atoms and of rotation in abundant molecules (Dalgarno and McCray 1972). More recently, the rates of fine-structure excitation of C^+ by H_2 and of C by H have been calculated by Chu and Dalgarno (1975*c*) and Yau and Dalgarno (1976), respectively. Cooling by CO rotational lines has been discussed by de Jong, Chu, and Dalgarno (1975) based upon the cross sections of Chu and Dalgarno (1975*c*) and Green and Thaddeus (1976). In our models, the cooling by rotational lines of H_2 follows directly from the statistical equilibrium calculation. This involves the transitions $J = 2 \rightarrow 0$ and $J = 3 \rightarrow 1$ only; in regions such as the ζ Oph cloud, the higher levels are not populated by thermal collisions and thus do not contribute to the heat loss. The optical thickness in the C^+ 156 μm line is not likely to be important in reducing the cooling in diffuse clouds. For a typical velocity dispersion of 5 km s^{-1}, the line absorption cross section averaged over the line profile is about 2×10^{-18} cm^2 so that $N(C^+) \approx 5 \times 10^{17}$ cm^{-2} is required to produce unit optical depth on the average. This corresponds typically to $N \approx 1.3 \times 10^{21}$ cm^{-2} and hence to a typical depth of $A_v \approx 1$ mag. At greater depths in regions exposed to normal radiation fields the carbon tends to be neutral or in molecular form anyway.

The presence of H_2 provides additional heat sources not considered by Dalgarno and McCray (1972). A newly formed H_2 molecule may emerge with significant kinetic energy (Silk 1973). Fluorescent dissociation of H_2 gives rise to a pair of energetic hydrogen atoms (Milgrom, Panagia, and Salpeter 1973; Stephens and Dalgarno 1973); for a typical ultraviolet radiation field, the yield is about 0.4 eV per atom pair, but it varies slightly with depth. In the adopted boundary radiation field, the average kinetic energy of the ejected electron in the photoionization of carbon is 1.06 eV. This quantity decreases somewhat with depth, as the more energetic photons are attenuated more rapidly by the grains. Heating due to cosmic ray and X-ray ionizations followed by secondary excitations and ionizations depends upon details of the energy-loss processes (Glassgold and Langer 1973; Cravens 1974). The process likely to dominate the heating of diffuse clouds is the photoemission of electrons from grain surfaces as suggested by Watson (1972) and re-examined by Jura (1976) and by de Jong (1977). In the present model, this heat source can be expressed in terms of the efficiency of photoemission, ϵ_g, and the rate at which energy is physically absorbed by the grains,

$$\frac{\Gamma_g}{\epsilon_g} = n(g) Q_v \pi r_g^2 \int_{\nu_0}^{\nu_L} \phi(\nu) h\nu \frac{\tau(\nu)}{\tau_v} (1 - \tilde{\omega}_\nu) e^{-k\tau(\nu)} d\nu , \quad (115)$$

where $\tau(\nu)/\tau_v$, k, and $\tilde{\omega}$ are tabulated in Table 1, and the quantity

$$n(g)Q_v\pi r_g^2 = 8 \times 10^{-22} n \qquad (116)$$

is derived from extinction measurements. Assuming that photoemission is efficient in the range $h\nu_0 = 10$ eV to $h\nu_L = 13.59$ eV and evaluating the integral as a function of depth, we obtain an expression for the heating rate,

$$\Gamma_g = 1.8 \times 10^{-25} \epsilon_g n I \exp(-2.304 A_v) \text{ ergs cm}^{-3} \text{ s}^{-1} . \qquad (117)$$

A plausible estimate for ϵ_g is 0.1.

Chemical heating (Dalgarno and Oppenheimer 1974) is an additional source in which energy released in exothermic chemical reactions is available to heat the gas. The effect is amplified when sequences of reactions form nearly closed cycles, such as those involving hydrocarbon radicals described above. In some cases this input may range from 35 to 100 eV per initiating reaction $C^+ + H_2 \rightarrow CH_2^+ + h\nu$. The energy derives ultimately from the photons which ionize C in the first place and ionize and dissociate CH_2 and CH_3, etc., to sustain the chemical cycle.

In the ζ Oph cloud model, heating by photoemission of electrons from grains dominates throughout, while the formation of hot H_2 is the next most important source. The cooling rate is controlled by fine-structure excitation of C^+ by H in the hot zone, but this mechanism is much less efficient at the lower temperatures and lower concentrations of H in the inner zone. In the inner zone the greatest contribution to the cooling is electron-impact excitation of C^+ because the fractional ionization remains roughly the same as in the outer region while the total density increases by a factor of 5. The remainder of the cooling is supplied by fine-structure transitions in neutral carbon excited by H and H_2. The total heating and cooling rates have been evaluated for the cloud model, and in an average sense they balance. In detail, however, the cooling rate exceeds the heating rate by about a factor of 5 throughout the outer region while heating exceeds cooling by about a factor of 2 in the interior. When the rates are weighted by the H_2 density and averaged over path length, the two averages agree at 4.5×10^{-23} ergs cm^{-3} s^{-1} when $\epsilon_g = 0.08$ in equation (117). The weighting follows the density of H_2 because it is the H_2 which is the empirical temperature indicator. This result suggests that with a more carefully determined continuous profile of temperature and density, the cloud model could be brought into a realistic thermal equilibrium consistent with observations. It appears likely that the heating and cooling processes identified above can account for the observed temperature.

V. DISCUSSION

Since the work of Hollenbach, Werner, and Salpeter (1971) on H_2 in interstellar clouds, many model calculations applicable to diffuse molecular clouds have been performed. The *Copernicus* observations (Spitzer *et al.* 1973; Spitzer, Cochran, and Hirshfeld 1974) of H_2 in many regions made it possible to study in detail the properties of these clouds. Glassgold and Langer (1974) presented isobaric cloud models which accounted for the average properties of the clouds rather well. In particular, they demonstrated that the average low-J rotational temperature, the molecular fraction, and the ionization balance of carbon could be reproduced in self-consistent fashion. In our attempt to explain many more observed quantities, we have not yet tried to treat the thermal balance correctly and simultaneously with the other equilibrium constraints. The cloud we have studied is apparently much denser than the models of Glassgold and Langer (1974), and as a result, both the heating and cooling rates may change more rapidly with depth than they found, thus allowing for a greater range of temperature through the cloud.

Following the suggestion that the higher rotational levels of H_2 are pumped by ultraviolet photons (Black and Dalgarno 1973*a*), Spitzer and Zweibel (1974) and Jura (1975*a*, *b*) have also calculated models to reproduce the rotational distributions. The difficulties encountered by Jura (1975*b*) in producing a good model of the level populations in the ζ Oph cloud have been removed by allowing temperature and density to vary with depth. That this is a more nearly correct approach is further substantiated by the success of our model in accounting for the atomic ionization equilibria, the molecular abundances, and the fine-structure populations of neutral carbon at the same time. The boundary rate of dissociation in Jura's (1975*b*) model for ζ Oph is about seven times that in our model. In Jura's model, radiation is incident upon one side, while in our model both sides are exposed to the same flux. Our model has a total linear extent of about $L = 2 \times 10^{18}$, so that the average density $\bar{n} = N/L \approx 600$ cm^{-3} is found to be very similar to the density of Jura's model, $n = 700$ cm^{-3}.

Hollenbach, Chu, and McCray (1976) have constructed models which combine a treatment of the molecular hydrogen data with a physical explanation of the origin of the clouds. They have noted that the stars used in the interstellar absorption line studies are often the very ones with considerable mass loss through strong stellar winds. The development of a wind-driven circumstellar shell provides a natural explanation of the high gas pressures inferred for many of the diffuse molecular clouds. This picture of diffuse clouds had been suggested earlier by Steigman, Strittmatter, and Williams (1975) who did not, however, consider the implications of the presence of molecular hydrogen. Regardless of the dynamical and evolutionary boundary conditions, the important physical processes will occur as we have described, as long as our assumption of a steady state is roughly valid. It will be interesting to see whether our modeling techniques can be used to draw conclusions about the dynamical states of the diffuse clouds. Clearly, the next step in increasing sophistication will be the integration into the model calculation of the detailed balance of heating and cooling along with stability considerations.

APPENDIX

RATES OF PHOTODESTRUCTION PROCESSES

Equilibrium abundances of about 100 neutral atoms, ions, and simple molecules are computed using a scheme of about 250 gas-phase reactions in addition to atomic photoionization and radiative recombination. The list of reactions derives largely from the work of Herbst and Klemperer (1973), except where indicated in the text. We have added a number of photodestruction processes, which are summarized in Table 8.

TABLE 8

RATES OF PHOTODESTRUCTION PROCESSES*

Process	Reactants	Products	a	b	Reference
1.....	H^-	$H + e$	3.36 (−8)	0.7094	1, 2
2.....	H_2	H + H	See text	...	...
3.....	H_2^+	$H + H^+$	2.57 (−10)	1.75	3
4.....	H_3^+	$H_2^+ + H$	7.9 (−9)	2.25	4, 5, 6, 7
5.....	H_3^+	$H_2 + H^+$	2.0 (−8)	1.84	
6.....	OH^+	...	1.2 (−12)	1.808	8
7.....	OH	O + H	1.5 (−10)	3.092	9, 10, 11
8.....	H_2O^+	...	0.1 times rate of 10	...	8
9.....	H_3O^+	...	0.1 times rate of 10	...	8
10.....	H_2O	OH + H	3.2 (−10)	1.677	12
11.....	CH	$CH^+ + e$	2.89 (−10)	2.75	13
12.....	CO	C + O	5.0 (−12)	3.0	14, 15
13.....	CO^+	...	5.0 (−12)	...	8
14.....	CH^+	$C^+ + H$	4.6 (−12)	2.95	14, 16
15.....	H_2CO	$CO + H_2$	4.39 (−10)	1.613	17, 18
16.....	H_2CO	CO + 2H	4.39 (−10)	1.613	17, 18
17.....	CH_2	CH + H	5.0 (−11)	1.72	19
18.....	CH_3	$CH + H_2$	3.0 (−11)	1.72	19
19.....	CH_3	$CH_2 + H$	3.0 (−11)	1.72	19
20.....	CH_4	$CH_3 + H$	1.59 (−10)	2.17	20
21.....	CH_4	$CH_2 + H_2$	4.78 (−10)	2.17	20
22.....	CH_4	$CH + H + H_2$	1.59 (−10)	2.17	20
23.....	CN	C + N	5.0 (−11)	1.72	14
24.....	CH	C + H	1.4 (−10)	1.544	14, 16, 21
25.....	O_2	O + O	3.3 (−10)	1.4	12
26.....	HCl	H + Cl	1.3 (−10)	1.457	22
27.....	HCl^+	$H^+ + Cl$	2.0 (−10)	1.5	22
28.....	H_2Cl^+	$HCl^+ + H$	3.2 (−10)	1.667	22
29.....	C_2	C + C	5.0 (−11)	1.72	8
30.....	C_2^+	$C^+ + C$	1.0 (−11)	1.72	8
31.....	C_2H	CH + C	1.4 (−10)	1.72	8
32.....	CH_3^+	$CH_2^+ + H$	1.0 (−9)	1.72	19†
33.....	CH_3^+	$CH^+ + H_2$	1.0 (−9)	1.72	19†
34.....	CH_2^+	$CH^+ + H$	1.67 (−9)	1.72	19
35.....	OH	$OH^+ + e$	1.6 (−12)	3.092	8
36.....	H_2O	$H_2O^+ + e$	2.1 (−11)	3.094	12
37.....	H_2CO	$H_2CO^+ + e$	8.0 (−11)	2.812	23
38.....	H_2CO	$HCO^+ + H + e$	1.4 (−11)	3.092	23
39.....	CH_2	$CH_2^+ + e$	1.0 (−9)	2.284	19
40.....	CH_3	$CH_3^+ + e$	1.0 (−10)	2.069	19
41.....	HCl	$HCl^+ + e$	3.3 (−11)	3.094	22
42.....	O_2	$O_2^+ + e$	6.2 (−12)	3.10	8
43.....	NH_3	$NH_2 + H$	5.0 (−10)	2.0	24
44.....	NH_3	$NH + H_2$	5.0 (−11)	2.0	24
45.....	HCO	H + CO	8.8 (−10)	1.613	8
46.....	HCN	CN + H	1.0 (−10)	1.80	8
47.....	NH	N + H	8.0 (−10)	2.0	8

* All photodestruction rates are written in the form

$$k_i = a_i \exp(-b_i A_v)\ \mathrm{s}^{-1},$$

where it is understood that the tabulated value of a_i is for the adopted radiation field of intensity $I = 1.0$.

† Recent calculations by Blint, Marshall, and Watson (1976) suggest a dissociation rate of CH_3^+ near 10^{-11} s^{-1}. The difficulty in explaining the measured CH^+ abundance is increased.

REFERENCES.—(1) Doughty *et al.* 1966; (2) Macek 1967; (3) Dunn 1968; (4) Stecher and Williams 1970; (5) Linsky 1970; (6) Kawaoka and Borkman 1971; (7) Conroy 1969; (8) Estimate; (9) Czarny, Felenbok, and Lefebvre-Brion 1971; (10) Easson and Pryce 1973; (11) Smith and Stella 1975; (12) Hudson 1971; (13) Walker and Kelly 1972; (14) Solomon and Klemperer 1972; (15) Myer and Samson 1970; (16) Smith, Liszt, and Lutz 1973; (17) Gentieu and Mentall 1970; (18) Glicker and Stief 1971; (19) Black, Dalgarno, and Oppenheimer 1975; (20) Strobel 1969; (21) Elander and Smith 1973; (22) Jura 1974*a*; (23) Warneck 1971; (24) Stief *et al.* 1972.

The rate of photodissociation or photoionization is

$$k_i = \int_{\nu_t}^{\nu_L} \phi(\nu)\sigma_i(\nu)d\nu\,, \tag{A1}$$

where $\phi(\nu)$ is the intensity of the radiation field at frequency ν, $\sigma_i(\nu)$ is the cross section of the process i in cm^2, and the limits of integration are generally the threshold frequency, ν_t, and the frequency of the Lyman limit of atomic hydrogen, ν_L. The photon intensity depends of course upon the boundary intensity, $\phi_0(\nu)$, and the solution of the radiation transfer problem. The solution has the form

$$\phi(\nu) = \phi_0(\nu) \exp\,[-k\tau(\nu)]\,, \tag{A2}$$

which may be written as a function of A_v given the relation (40). The rates calculated from equation (A1) are all evaluated over a range of depths and then approximated by a function of the form

$$k_i = a_i \exp\,(-b_i A_v)\,. \tag{A3}$$

The tabulated values of a_i are appropriate for $I = 1.0$ in equation (107), and all rates are directly proportional to I. The only sources of opacity in the depth dependences are those due to grains, with the exception of the photoionization of carbon and photodissociation of H_2 and HD.

Where available, measured or calculated cross sections were used in the evaluation of equation (A1). When photodissociation depends upon line absorptions, as in predissociation, the process may be evaluated in terms of an effective oscillator strength, $f_{\rm eff}$. Since the intensity will vary insignificantly over the profile of an optically thin line, and since the effective oscillator strengths tend to be poorly determined anyway, it is usually adequate to express the rate of a predissociation as

$$k \approx \phi(\nu_0) \int \sigma(\nu)d\nu \tag{A4}$$

$$= \phi(\nu_0) \frac{\pi e^2}{mc} f_{\rm eff}\,. \tag{A5}$$

The references listed in Table 8 usually contain data useful in estimating rates, but may not always contain explicit cross sections or oscillator strengths.

TABLE 9

PHOTOIONIZATION RATES*

Species	Threshold (Å)	a_i	b_i	Reference
Li.....	2300	2.08 (−10)	1.939	1, 2
C.....	1110	1.31 (−10)	2.416	3, 4, This paper
Na.....	2413	5.60 (−12)	1.950	5
Mg.....	1622	4.45 (−11)	1.435	6, 7, 8, 9
Al.....	2071	1.38 (−9)	1.824	10, 11
Si.....	1521	1.20 (−9)	1.622	10
P.....	1129	3.36 (−10)	2.524	7
S.....	1197	7.20 (−10)	2.390	12
Cl.....	956	9.90 (−11)	3.094	13, 7
K.....	2856	3.51 (−11)	1.829	14, 15, 16, 5
Ca.....	2028	3.12 (−10)	1.890	17, 18
Ca^+.....	1044	1.72 (−12)	2.862	19
Ti.....	1814	2.15 (−10)	1.678	7
Mn.....	1668	4.47 (−11)	1.429	7
Fe.....	1569	1.17 (−10)	1.536	20

* All photoionization rates are written in the form

$$k_i = a_i \exp\,(-b_i A_v)\ {\rm s}^{-1}\,,$$

where it is understood that the tabulated value of a_i is for the adopted radiation field of intensity $I = 1.0$.

REFERENCES.—(1) Caves and Dalgarno 1972; (2) Hudson and Carter 1967*a*; (3) Bates and Seaton 1949; (4) Henry 1970; (5) Weisheit 1972; (6) Bates and Altick 1973; (7) McGuire 1968; (8) Dubau and Wells; (9) Ditchburn and Marr 1953; (10) Conneely, Smith, and Lipsky 1970; (11) Burgess, Field, and Michie 1960; (12) Chapman and Henry 1971; (13) Peach 1967; (14) Marr and Creek 1968; (15) Hudson and Carter 1966; (16) Hudson and Carter 1967*b*; (17) Carter, Hudson, and Breig 1971; (18) McIlrath and Sandemann 1972; (19) Black, Weisheit, and Laviana 1972; (20) Kelly 1972.

The adopted photoionization rates for abundant atoms and ions having ionization potentials less than 13.6 eV are listed in Table 9. Similar rates have been presented by de Boer, Koppenaal, and Pottasch (1973). Agreement with our rates is good for a comparable radiation field.

Rates of radiative recombination for atomic species are adopted from Aldrovandi and Pequignot (1973), Seaton (1951), Caves and Dalgarno (1972), and Weisheit (1973).

REFERENCES

Aannestad, P. A., and Field, G. B. 1973, *Ap. J. (Letters)*, **186**, L29.
Abt, H. A., and Biggs, E. S. 1972, *Bibliography of Stellar Radial Velocities* (Tucson: Kitt Peak National Observatory).
Aldrovandi, S. M. V., and Pequignot, D. 1973, *Astr. Ap.*, **25**, 137.
Allen, M., and Robinson, G. W. 1976, *Ap. J.*, **207**, 745.
Allison, A. C., and Dalgarno, A. 1967, *Proc. Phys. Soc.*, **90**, 609.
Barlow, M. J., and Silk, J. 1976, *Ap. J.*, **207**, 131.
Bates, D. R., and Seaton, M. J. 1949, *M.N.R.A.S.*, **109**, 698.
Bates, D. R., and Spitzer, L. 1951, *Ap. J.*, **113**, 441.
Bates, G. N., and Altick, P. L. 1973, *J. Phys.*, **B6**, 653.
Black, J. H., and Dalgarno, A. 1973*a*, *Ap. J. (Letters)*, **184**, L101.
———. 1973*b*, *Ap. Letters*, **15**, 79.
———. 1976, *Ap. J.*, **203**, 132.
Black, J. H., Dalgarno, A., and Hartquist, T. 1977, in preparation.
Black, J. H., Dalgarno, A., and Oppenheimer, M. 1975, *Ap. J.*, **199**, 633.
Black, J. H., Weisheit, J. C., and Laviana, E. 1972, *Ap. J.*, **177**, 567.
Bless, R. C., and Savage, B. D. 1972, *Ap. J.*, **171**, 293.
Blint, R. J., Marshall, R. F., and Watson, W. D. 1976, *Ap. J.*, **205**, 634.
Burgess, A., Field, G. B., and Michie, R. W. 1960, *Ap. J.*, **131**, 529.
Carruthers, G. R. 1970, *Ap. J. (Letters)*, **161**, L81.
Carter, V. L., Hudson, R. D., and Breig, E. L. 1971, *Phys. Rev.*, **A4**, 821.
Caves, T. C., and Dalgarno, A. 1972, *J. Quant. Spectrosc. Rad. Transf.*, **12**, 1539.
Chaffee, F., and Lutz, B. L. 1977, *Ap. J.*, **213**, 394.
Chandrasekhar, S. 1960, *Radiative Transfer* (New York: Dover).
Chapman, R. D., and Henry, R. J. W. 1971, *Ap. J.*, **168**, 169.
Chu, S.-I, and Dalgarno, A. 1975*a*, *Ap. J.*, **199**, 637.
———. 1975*b*, *J. Chem. Phys.*, **63**, 2115.
———. 1975*c*, *Proc. Roy. Soc.*, **A342**, 191.
Conneely, M. J., Smith, K., and Lipsky, L. 1970, *J. Phys.*, **B3**, 493.
Conroy, H. 1969, *J. Chem. Phys.*, **51**, 3979.
Cravens, T. 1974, Ph.D. thesis, Harvard University.
Crutcher, R. M., and Watson, W. D. 1976, *Ap. J. (Letters)*, **203**, L123.
Czarny, J., Felenbok, P., and Lefebvre-Brion, H. 1971, *J. Phys.*, **B4**, 124.
Dalgarno, A. 1976, in *Atomic Processes and Applications*, ed. P. G. Burke and B. L. Moiseiwitsch (Amsterdam: North-Holland), p. 110.
Dalgarno, A., and Black, J. H. 1976, *Rept. Progr. Phys.*, **39**, 573.
Dalgarno, A., Black, J. H., and Weisheit, J. C. 1973, *Ap. Letters*, **14**, 77.
Dalgarno, A., de Jong, T., Oppenheimer, M., and Black, J. H. 1974, *Ap. J. (Letters)*, **192**, L37.
Dalgarno, A., Henry, R. J. W., and Roberts, C. S. 1966, *Proc. Phys. Soc.*, **88**, 611.
Dalgarno, A., and McCray, R. 1972, *Ann. Rev. Astr. Ap.*, **10**, 375.
———. 1973, *Ap. J.*, **181**, 95.
Dalgarno, A., and Oppenheimer, M. 1974, *Ap. J.*, **192**, 597.
Dalgarno, A., and Stephens, T. L. 1970, *Ap. J. (Letters)*, **160**, L107.
Davies, R. D., and Matthews, H. E. 1972, *M.N.R.A.S.*, **156**, 253.
de Boer, K. S., Koppenaal, K., and Pottasch, S. R. 1973, *Astr. Ap.*, **28**, 145.
de Boer, K. S., and Morton, D. E. 1974, *Astr. Ap.*, **37**, 305.
de Boer, K. S., Morton, D. C., Pottasch, S. R., and York, D. G. 1974, *Astr. Ap.*, **31**, 405.
de Jong, T. 1977, *Astr. Ap.*, **55**, 137.
de Jong, T., Chu, S.-I, and Dalgarno, A. 1975, *Ap. J.*, **199**, 69.
diGeorgio, V. E., and Robinson, G. W. 1959, *J. Chem. Phys.*, **31**, 1678.
Ditchburn, R. W., and Marr, G. V. 1953, *Proc. Phys. Soc.*, **A66**, 665.
Doughty, N. A., Fraser, P. A., and McEachran, R. P. 1966, *M.N.R.A.S.*, **132**, 255.
Dubau, J., and Wells, J. 1973, *J. Phys.*, **B6**, L31.
Dunn, G. H. 1968, *Phys. Rev.*, **172**, 1.
Easson, I., and Pryce, M. H. L. 1973, *Canadian J. Phys.*, **51**, 518.
Elander, N., and Smith, W. H. 1973, *Ap. J.*, **184**, 663.
Field, G. B. 1974, *Ap. J.*, **187**, 453.
Gentieu, E. P., and Mentall, J. E. 1970, *Science*, **169**, 681.
Georgelin, Y. P., and Georgelin, Y. M. 1970, *Astr. Ap.*, **6**, 349.
Glassgold, A. E., and Langer, W. D. 1973, *Ap. J.*, **186**, 859.
———. 1974, *Ap. J.*, **193**, 73.
———. 1976, *Ap. J.*, **206**, 85.
Glicker, S., and Stief, L. J. 1971, *J. Chem. Phys.*, **54**, 2852.
Green, S. 1975, *J. Chem. Phys.*, **62**, 2271.
Green, S., and Thaddeus, P. 1976, *Ap. J.*, **205**, 766.
Habing, H. J. 1968, *Bull. Astr. Inst. Netherlands*, **19**, 421.
Henry, R. J. W. 1970, *Ap. J.*, **161**, 1153.
Herbig, G. H. 1968, *Zs. f. Ap.*, **68**, 243.
Herbst, E., and Klemperer, W. 1973, *Ap. J.*, **185**, 505.
Herbst, E., Schubert, J. G., and Certain, P. R. 1977, *Ap. J.*, **213**, 696.
Herzberg, G. 1961, *Proc. Roy. Soc.*, **A262**, 291.
Herzberg, G., Lagerqvist, A., and Malmberg, C. 1969, *Canadian J. Phys.*, **47**, 2735.
Hollenbach, D. J., Chu, S.-I, and McCray, R. 1976, *Ap. J.*, **208**, 458.
Hollenbach, D. J., and Salpeter, E. E. 1970, *J. Chem. Phys.*, **53**, 79.
———. 1971, *Ap. J.*, **163**, 155.
Hollenbach, D. J., Werner, M. W., and Salpeter, E. E. 1971, *Ap. J.*, **163**, 165.
Hudson, R. D. 1971, *Rev. Geophys. Space Phys.*, **9**, 306.
Hudson, R. D., and Carter, V. L. 1966, *Phys. Rev.*, **139**, 1426.
———. 1967*a*, *J. Opt. Soc. Am.*, **57**, 651.
———. 1967*b*, *J. Opt. Soc. Am.*, **57**, 1471.
Huntress, W. T. 1977, *Ap. J. Suppl.*, **33**, 495.
Johnson, B. R., and Secrest, D. 1968, *J. Chem. Phys.*, **48**, 4082.
Johnson, H. L., and Borgman, J. 1963, *Bull. Astr. Inst. Netherlands*, **17**, 115.
Jura, M. 1974*a*, *Ap. J. (Letters)*, **190**, L33.
———. 1974*b*, *Ap. J.*, **191**, 375.
———. 1975*a*, *Ap. J.*, **197**, 575.
———. 1975*b*, *Ap. J.*, **197**, 581.
———. 1976, *Ap. J.*, **204**, 12.
Jura, M., and Dalgarno, A. 1971, *Astr. Ap.*, **14**, 243.
Kawaoka, K., and Borkman, R. F. 1971, *J. Chem. Phys.*, **54**, 4234.
Kelly, H. P. 1972, *Phys. Rev.*, **A46**, 1048.
Linsky, J. L. 1970, *Solar Phys.*, **11**, 198.
Macek, J. 1967, *Proc. Phys. Soc.*, **92**, 365.
Marenin, I. R., and Johnson, H. R. 1970, *J. Quant. Spectrosc. Rad. Transf.*, **10**, 305.
Marr, G. V., and Creek, D. M. 1968, *Proc. Roy. Soc.*, **A304**, 233.
McDowell, M. R. C. 1961, *Observatory*, **81**, 240.

McGuire, E. J. 1968, *Phys. Rev.*, **175**, 20.
McGuire, P., and Micha, D. A. 1972, *Internat. J. Quant. Chem., Symp. No. 6*, p. 111.
McIlrath, T., and Sandemann, R. J. 1972, *J. Phys.*, **B5**, L217.
Milgrom, M., Panagia, N., and Salpeter, E. E. 1973, *Ap. Letters*, **14**, 73.
Moraal, H., and McCourt, F. R. 1972, *Physica*, **60**, 73.
Morton, D. C. 1974, *Ap. J. (Letters)*, **193**, L35.
———. 1975, *Ap. J.*, **197**, 85.
Myer, J. A., and Samson, J. A. R. 1970, *J. Chem. Phys.*, **52**, 266.
Nishimura, S. 1968, *Ann. Tokyo Astr. Obs.*, **11**, 33.
O'Donnell, E. J., and Watson, W. D. 1974, *Ap. J.*, **191**, 89.
Oppenheimer, M., and Dalgarno, A. 1974, *Ap. J.*, **187**, 231.
Peach, G. 1967, *Mem. R.A.S.*, **71**, 29.
Rodgers, C. D., and Williams, A. P. 1974, *J. Quant. Spectrosc. Rad. Transf.*, **14**, 319.
Rogerson, J. B., and York, D. G. 1973, *Ap. J. (Letters)*, **186**, L95.
Roux, F., Cerny, D., and d'Incan, J. 1976, *Ap. J.*, **204**, 940.
Sandell, G., and Mattila, K. 1975, *Astr. Ap.*, **42**, 357.
Seaton, M. J. 1951, *M.N.R.A.S.*, **111**, 368.
Silk, J. 1973, *Pub. A.S.P.*, **85**, 704.
Smith, A. M. 1973, *Ap. J. (Letters)*, **179**, L11.
Smith, W. H. 1969, *Ap. J.*, **156**, 791.
Smith, W. H., Liszt, H. S., and Lutz, B. L. 1973, *Ap. J.*, **153**, 69.
Smith, W. H., and Stella, G. 1975, *J. Chem. Phys.*, **63**, 2395.
Smith, W. H., and Zweibel, E. G. 1976, *Ap. J.*, **207**, 758.
Snow, T. P. 1975, *Ap. J. (Letters)*, **202**, L87.
———. 1976, *Ap. J. (Letters)*, **204**, L127.
Solomon, P. M., and Klemperer, W. 1972, *Ap. J.*, **178**, 389.
Solomon, P. M., and Werner, M. W. 1971, *Ap. J.*, **165**, 41.
Spindler, R. J. 1965, *J. Quant. Spectrosc. Rad. Transf.*, **5**, 165.
Spitzer, L. 1968, *Diffuse Matter in Space* (New York: Interscience).
Spitzer, L., Cochran, W. D., and Hirshfeld, A. 1974, *Ap. J. Suppl.*, **28**, 373.
Spitzer, L., Drake, J. F., Jenkins, E. B., Morton, D. C., Rogerson, J. B., and York, D. G. 1973, *Ap. J. (Letters)*, **181**, L116.
Spitzer, L., and Jenkins, E. B. 1975, *Ann. Rev. Astr. Ap.*, **13**, 133.
Spitzer, L., and Morton, W. A. 1976, *Ap. J.*, **204**, 731.
Spitzer, L., and Zweibel, E. G. 1974, *Ap. J. (Letters)*, **191**, L127.
Stecher, T. P., and Williams, D. A. 1967, *Ap. J. (Letters)*, **149**, L29.
———. 1970, *Ap. Letters*, **7**, 59.
Steigman, G., Strittmatter, P. A., and Williams, R. E. 1975, *Ap. J.*, **198**, 575.
Stephens, T. L., and Dalgarno, A. 1972, *J. Quant. Spectrosc. Rad. Transf.*, **12**, 569.
———. 1973, *Ap. J.*, **186**, 165.
Stief, L. J., Donn, B., Glicker, S., Gentieu, E. P., and Mentall, J. E. 1972, *Ap. J.*, **171**, 21.
Strobel, D. F. 1969, *J. Atm. Sci.*, **26**, 906.
Walker, T. E. H., and Kelly, H. P. 1972, *Chem. Phys. Letters*, **16**, 511.
Walmsley, M. 1973, *Astr. Ap.*, **25**, 129.
Warneck, P. 1971, *Zs. f. Naturforschung*, **26a**, 2047.
Watson, W. D. 1972, *Ap. J.*, **176**, 103; Addendum, *ibid.*, **176**, 271.
———. 1973, *Ap. J. (Letters)*, **182**, L73.
———. 1974, *Ap. J.*, **188**, 35.
Weisheit, J. C. 1972, *Phys. Rev.*, **B5**, 1621.
———. 1973, *Ap. J.*, **185**, 877.
Wright, E. L., and Morton, D. C. 1977, *Ap. J.*, in press.
Witt, A. N., and Lillie, C. F. 1973, *Astr. Ap.*, **25**, 392.
Wolken, G., Miller, W. H., and Karplus, M. 1972, *J. Chem. Phys.*, **56**, 4930.
Yau, A. W., and Dalgarno, A. 1976, *Ap. J.*, **206**, 652.
York, D. G., Drake, J. F., Jenkins, E. B., Morton, D. C., Rogerson, J. B., and Spitzer, L. 1973, *Ap. J. (Letters)*, **182**, L1.
York, D. G., and Rogerson, J. B. 1976, *Ap. J.*, **203**, 378.

J. H. BLACK: School of Physics and Astronomy, University of Minnesota, Minneapolis, MN 55455

A. DALGARNO: Center for Astrophysics, Cambridge, MA 02138